ISSN 1028-334X, Doklady Earth Sciences, 2025, Vol. 522:50. © Pleiades Publishing, Ltd., 2025.

LANDSCAPES AND LANDFORMS OF SIBERIA

Giant Pleistocene Ice-Dammed Lakes of Gorny Altai

I. D. Zolnikov[a] and E. V. Deev[b,*]

[a]*Sobolev Institute of Geology and Mineralogy, Siberian Branch, Russian Academy of Sciences, Novosibirsk, 630090 Russia*

[b]*Trofimuk Institute of Petroleum Geology and Geophysics, Siberian Branch, Russian Academy of Sciences, Novosibirsk, 630090 Russia*

**e-mail: DeevEV@ipgg.sbras.ru*

Received March 11, 2025; revised March 15, 2025; accepted March 20, 2025

Abstract—Middle-Late Pleistocene giant ice-dammed paleolakes occupied in the Pleistocene Uimon (lake volume 450 km^3), Kurai (229 km^3), Chuya (838 km^3), and Kan-Yabogan basins of Gorny Altai, southern Siberia. The lake volumes were estimated along the contours of wave-cut terraces, and Kurai and Chuya lakes taken together turned out to fit the 1056 km^3 size of a temporary paleolake, which formed in the Biya-Barnaul segment of the Ob Valley due to flooding of the Fore-Altai plain by megafloods. However, no megaflood events were associated with breakthrough of rockfall-dammed lakes in the Chuya and Katun valleys or small ice-dammed lakes in Gorny Altai. Abrupt discharge of lakes through broken ice, landslide, or moraine dams could cause floods in the Chuya and Katun valleys about 18–14 ka ago, but their volumes and the effects of erosion, sediment transport, and terrain sculpturing were far inferior to those of the older glacial megafloods.

Keywords: glaciation, ice-dammed lake, megaflood, Gorny Altai, Fore-Altai plain

DOI: 10.1134/S1028334X2560642X

INTRODUCTION

Geological evidence of giant Pleistocene ice-dammed lakes is of special importance in stratigraphic correlations and paleogeographic reconstructions for Gorny Altai (Fig. 1). The timing of large lakes in intermontane basins barred with glaciers can place age constraints on largest glacier outburst floods (megaflood) deposition in the Chuya and Katun valleys resulting from catastrophic events of lake discharge.

The area of Gorny Altai affected by Pleistocene glaciation comprises zones of glacial erosion and till (moraine) deposition (Fig. 1). In Quaternary time, some intermontane basins accommodated ice while others were dammed with glaciers at the exit, became filled with water, and turned into lakes. Ice-dammed lakes existed in the large Chuya, Kurai, Uimon, and Kan-Yabogan basins (Fig. 1). As the glaciers degraded, the ice dams broke down, and water rushed from the lakes producing megafloods, which were major agents in sculpturing the Quaternary landforms in Gorny Altai and in the Fore-Altai plain. However, the contributions of damlakes to the process were different: for instance, the moderate amount of material discharged from Kan-Yabogan lake into the Charysh River Valley left almost no traces in landform.

KAN-YABOGAN ICE-DAMMED LAKE

The large Kan-Yabogan paleolake near the present location of Ust'-Kan Villadge (Fig. 2) formed when a glacier barred the Charysh and Kan rivers at the confluence, where the Kan-Yabogan Depression narrows down to few hundred meters. The existence of a former glacier is recorded in brown to ochreous till which overlies eluvium over Paleozoic gray schists [3]. The top of the schist layer bears signatures of glacial deformation as folds and diapirs penetrating into the till layer (Fig. 3). Some diapirs are truncated by low-angle glacial thrusts, and their top parts are displaced laterally to different distances. For instance, the 4 m long and 40 cm thick sheet of gray eluvial debris standing out against brown till (Fig. 4) was detached from the glacier-bed deposits and entrained with the motion of the Ust'Kan till.

The boundary of the Ust'-Kan paleoglacier (Fig. 2) is traceable along the limits of glacial boulders and blocks of Devonian plagioclase porphyritic rocks (Fig. 5), which are widespread within the territory of the Ust'-Kan Villadge and a few kilometers around. Judging by the presence of Devonian porphyritic bedrock in the Kutergen River valley [4], a left tributary of the Charysh River near Ust'-Kan Villadge (Fig. 2), the glacier advanced into the Kan-Yabogan Depression along the Kutergen River.

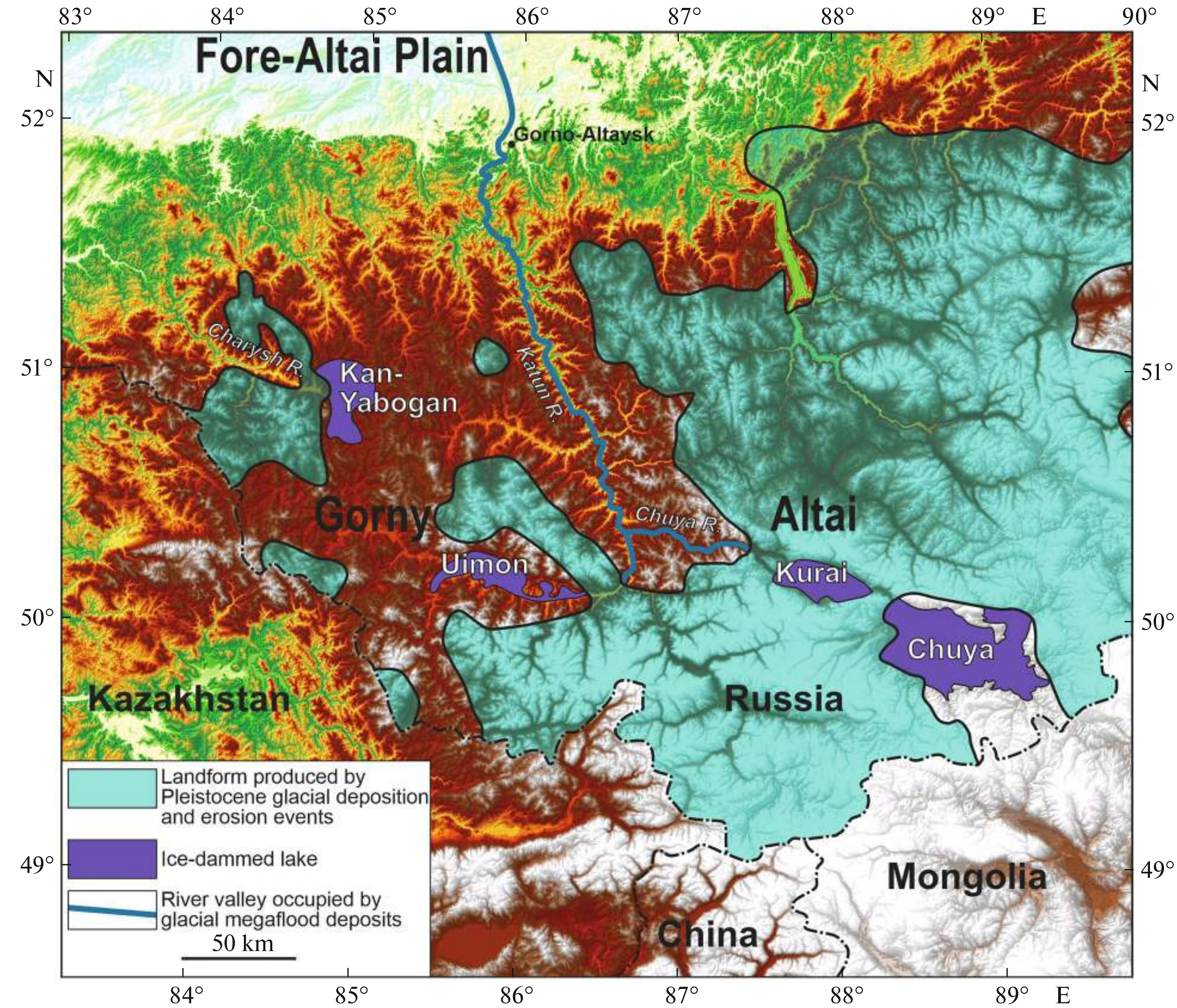

Fig. 1. Zone of Pleistocene glaciation in Gorny Altai, according [1, 2].

Lacustrine deposition is especially well evident in sands stripped in a quarry 3 km southwest of Yakonur Village (Fig. 6a). The quarry wall exposes eight sedimentary units (top to bottom): 0.5 m thick modern soil (Unit 1); 1 m of aeolian sand (Unit 2); two layers of ≤0.3 m thick buried soil (units 3 and 5) separated by 0.5 m of aeolian sand (Unit 4); 0.2 m thick sand cemented with carbonate material (Unit 6) which was formed while lacustrine sediments were drying; 4.1 m thick laminated lacustrine sand (Unit 7); lacustrine sand, up to 7.1 m of visible thickness (Unit 8), with less prominent lamination than in Unit 7, and with a whitish band in the top (Fig. 6b). Judging by the ~11 m thickness of the lacustrine sequence, the lake was deep enough during the deposition.

Units 7 and 8 are separated by a weakly expressed angular unconformity that may trace a seismic event. The area was apparently involved into tectonic activity after the lake had dried out, as one may infer from steeply dipping (~60°) reverse faults in the slope. Those faults, which hardly could be associated with landslides. The reverse slip geometry and minor displacements bending of sand lamination along the faults record the seismic origin of the soft-sediment deformation structures [5–7]. The geochronological and paleontological age constraints for the lacustrine sequence are as yet unavailable in the absence of fauna and organic remains, but a Pleistocene age of the paleolake can be inferred from the presence of a 3 m thick aeolian sand layer with two buried soils.

Lacustrine sands cover the whole bottom of the Kan-Yabogan Depression. Aeolian sands exposed in small quarries or silo pits reach 1.5 m in thickness and enclose two dark gray buried soils (at 0.5–0.6 m and 1.0–1.1 m below the ground surface). They lie over lacustrine sands stripped to a depth of 1.5 m, which

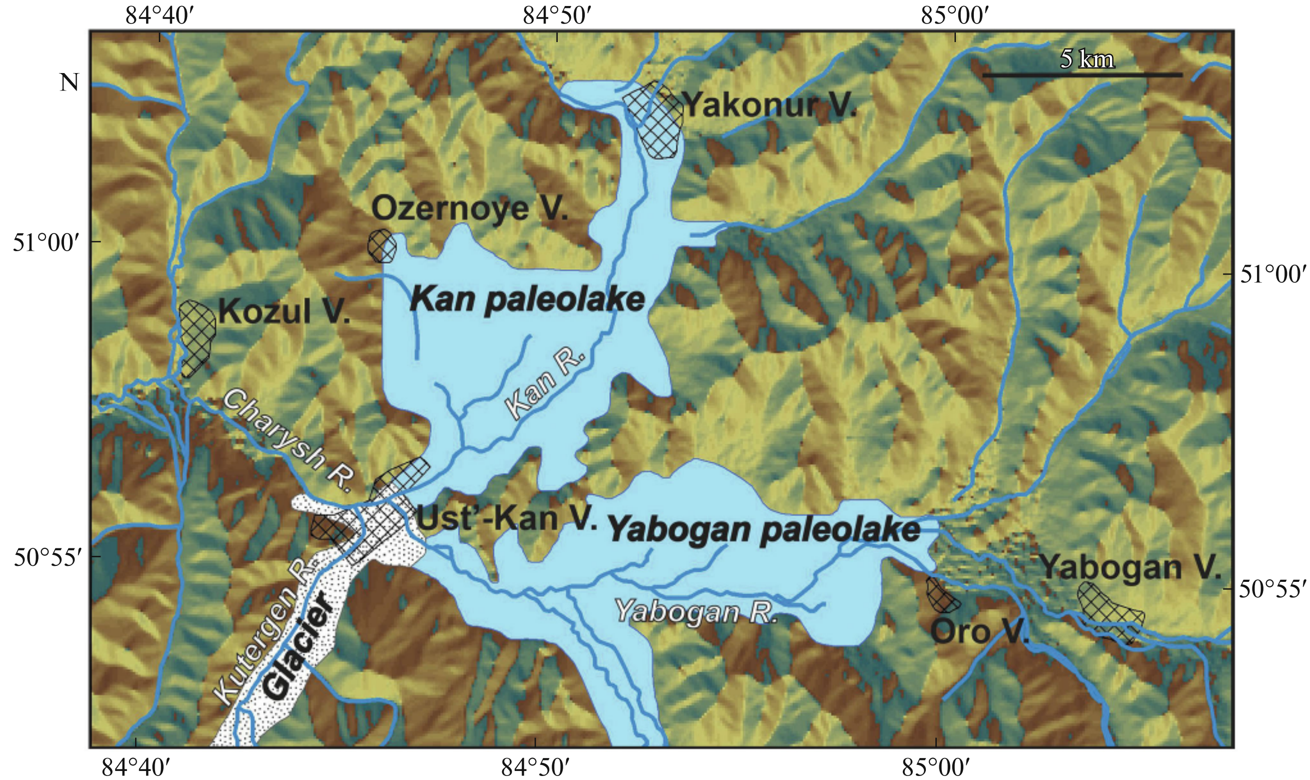

Fig. 2. Kan-Yabogan paleolake and its ice dam.

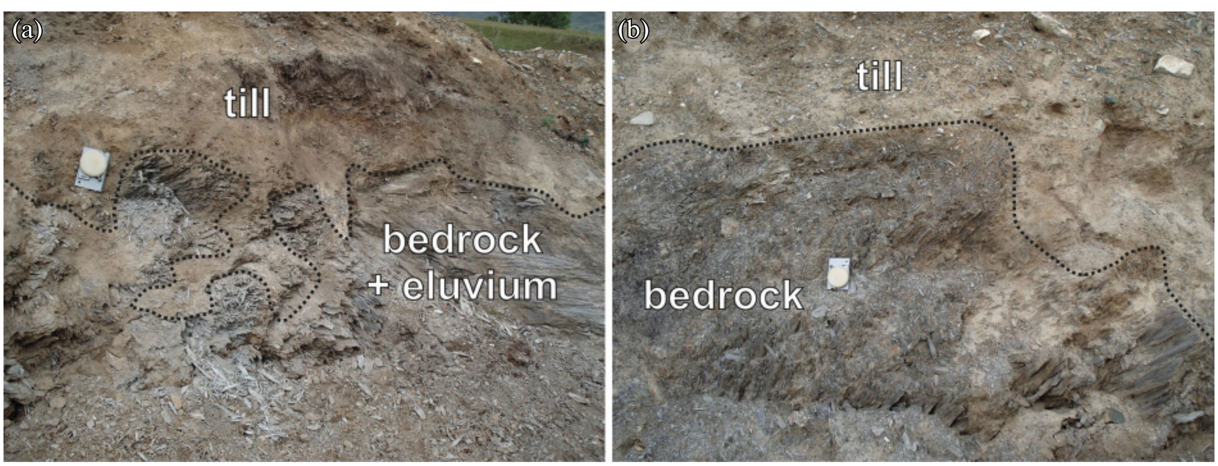

Fig. 3. Signatures of glacial deformation in the bed of the Ust'-Kan till: folds (left panel) and a truncated diapir (right panel). Compass is for scale.

contain a layer of angular granule with carbonate cement on the top. Excavation pits on the periphery of the Kan-Yabogan Basin expose lacustrine sand and silt sediments with various deformation structures, as well as colluvium (Fig. 7). These structures hardly can result from degradation of ground ice, because the size of recumbent folds often exceeds 5 m while aligned flame-like intrusions appear over long distances of tens or even hundreds of meters. The sediments contain coexisting mudflow and fluvial structures, which indicates high rates and large extent of the processes of their formation. The mudflow structures of this kind formed when lakes discharged rapidly through broken dams [8] and the water flushed sediments on the lake sides, forming a mud cover, wich had leveled the landform at the periphery of the lake basin. Mudflow

Fig. 4. Gray eluvial debris (glacier bed) sandwiched between brown diamictites (till).

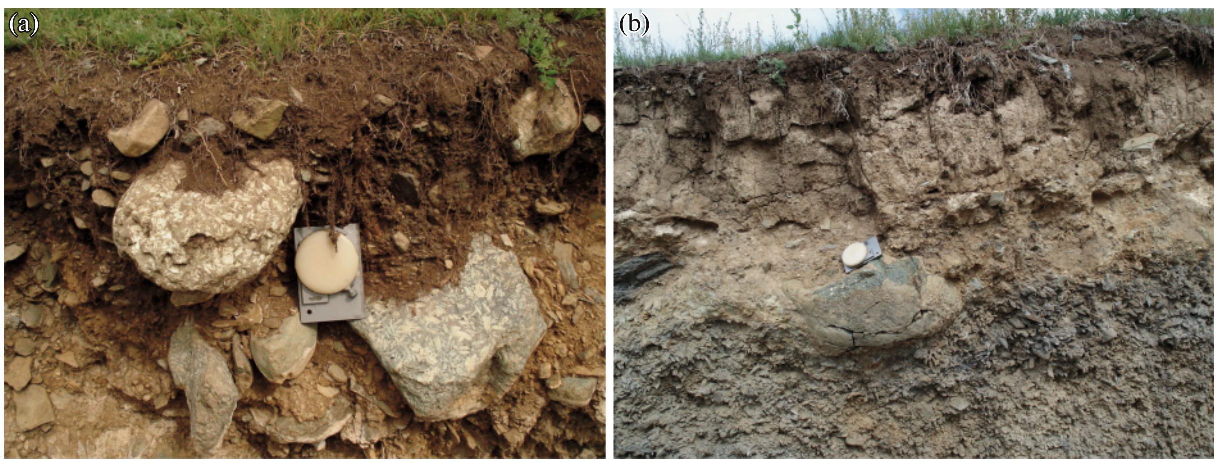

Fig. 5. Glacial boulders of Devonian plagioclase porphyritic rocks in the Ust'-Kan till. Compass is for scale.

deposits are widespread along the margins of the Uimon and Chuya intermontane basins (see below).

Note that the mudflow sediments disappear abruptly downstream of the Ust'-Kan till field along the Charysh River, where coarse gravels build a staircase of four above-floodplain terraces [9], including three Late Pleistocene ones. There are no terraces upstream of the Ust'-Kan Villadge. Therefore, the gravels downstream of the Ust'-Kan till were most likely deposited by flood associated with the breakthrough of ice dam and discharge of the lake. They rather quickly, sinking beneath subaerial sediments. Therefore, the flood from Kan-Yabogan damlake were less voluminous than those from other such lakes.

UIMON, KURAI, AND CHUYA ICE-DAMMED LAKES

Uimon damlake occupied the Uimon Basin in the upper reaches of the Katun River (Fig. 1), with its ice dam downstream of the Akkem River, a right tributary of the Katun. The glacier left a till which rises tens of meters high above the Katun level (Fig. 8). The lake level could reach an elevation of 1300 m asl and the water volume exceeded 450 km^3, as inferred from reliably identified landforms and from the thickness of lacustrine sediments [9]. However, the size of the ice dam, as well as the depth and volume of the paleolake, remain worse constrained than the respective parameters of the Kurai-Chuya paleolimnic system.

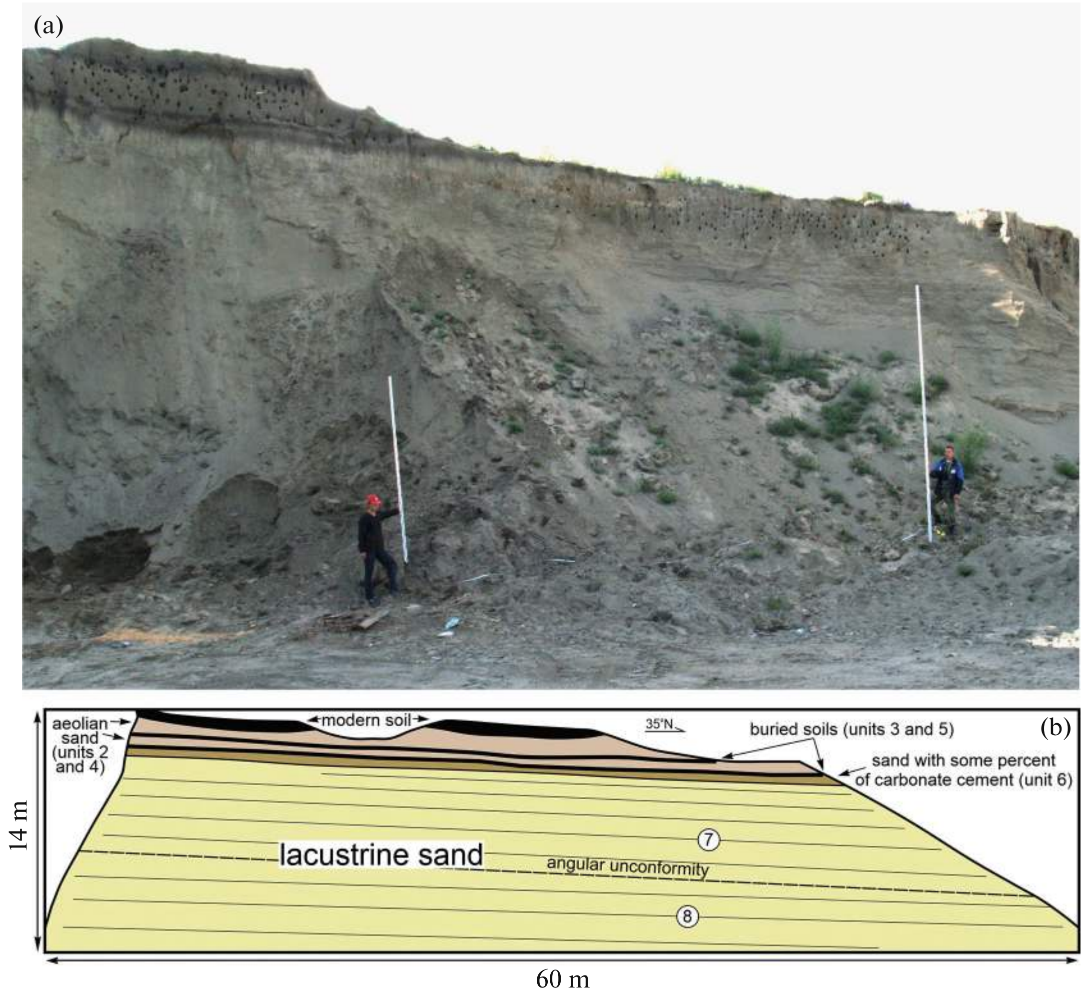

Fig. 6. Sand quarry in the Kan-Yabogan paleolake sediments. (a) outcrop fragment; (b) cross section.

The catastrophic lake drainage event is recorded by a coarse gravel downstream of the till complex along the Katun River and by an extensive field of giant current ripples in the eastern Uimon Basin. Outcrops in this basin part and in smaller basins downstream expose easily spotted megaflood facies (Fig. 9a), while mudflow deposits occur along the basin margins (Fig. 9b).

The available age constraints of Uimon ice-dammed lake are limited to a single 101 ± 9 ka optically stimulated luminescence (OSL) date of its sediments [11]. The dated sample was collected in an outcrop of lacustrine deposits, 12 m of visible thickness (top and bottom buried), in the eastern margin of the Uimon Basin. The sediments interpreted as lake shore facies are exposed in two closely spaced road excavations: *a* ~100 m long silt layer with nearly horizontal 5–10 cm thick sand and angular granule interbeds (Fig. 10a) and a sand and angular pebble with lenticular, parallel, or cross bedding (Fig. 10b). Presumably, 23 m thick alternating Late Pleistocene lacustrine sand, silt, clay, and pebble were stripped in a borehole in the central part of the Uimon Basin [12].

Not much is known either about the Kurai and Chuya paleolimnic systems, in spite of a long history of studies. Geological data from the borehole-5576 in the northwestern Chuya Basin reveal five cyclites in the 140 m thick Quaternary sequence. Each cycle consists of two units [13]: pebble (thickness 7–30 m) and clay (7–15 m), which were deposited, respectively, in subaerial interglacial conditions and on the bottom of ice-dammed lakes. The thickness and number of cycles stripped in boreholes decrease successively eastward to the basin periphery: three near Koshagach Village, two near Tobeler Village, and one or no such cycles near the basin margin, where only coarse shore facies are often present. The coarse sediments consist of alternating boulder-pebble, pebble-granule-clay, or sand layers, up to 5–8 pairs, correlated with the deposition cycles in the basin center [13]. This cyclicity confirms the existence of several Quaternary glaciations, with ice-dammed lakes in the Chuya Basin.

Fig. 7. Outcrop of mudflow deposits formed during rapid discharge of Kan-Yabogan ice-dammed lake.

Fig. 8. Till exposed in the Katun right bank, 10 km downstream of Akkem River.

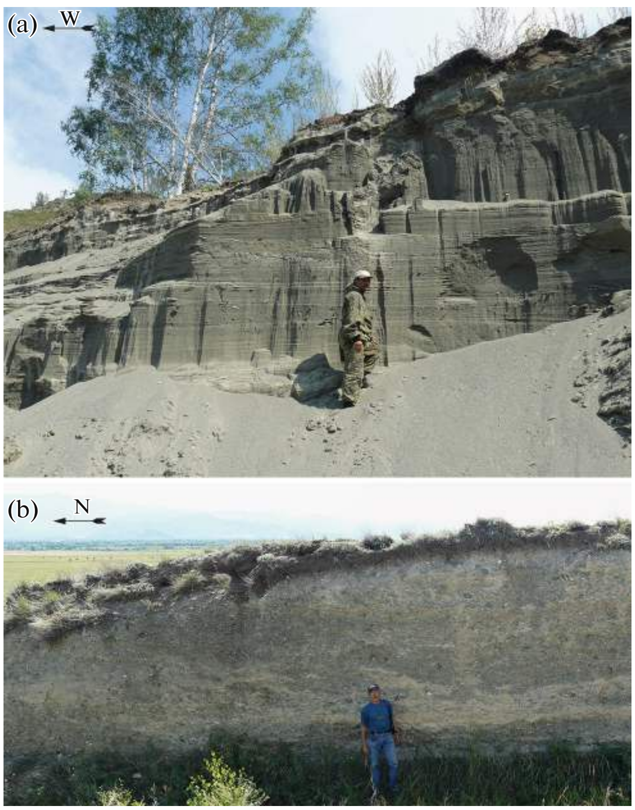

Fig. 9. Deposits that represent the lake drainage event in the Uimon Basin. (a) megaflood parallel-laminated sands and angular granule; (b) mudflow deposits along the northern basin margin.

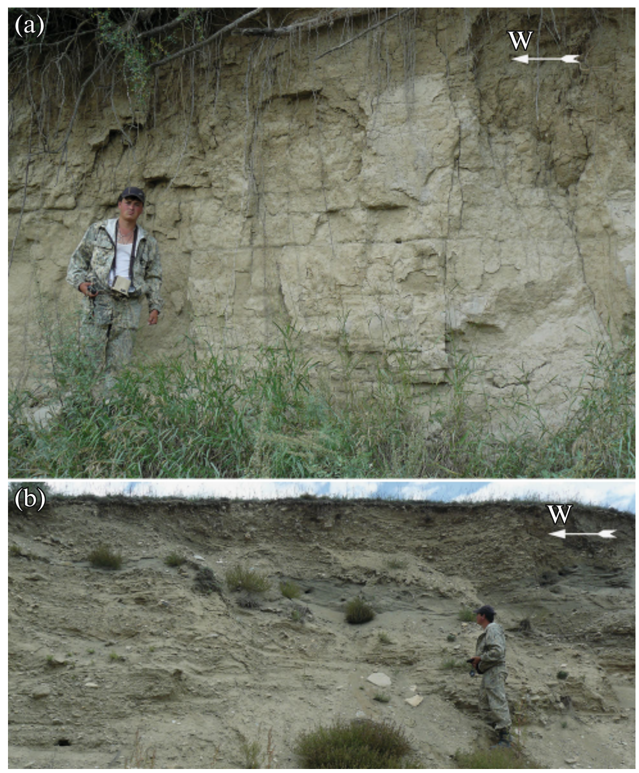

Fig. 10. Exposed near-shore deposits of Uimon paleolake. (a) silt with sand and angular granule interbeds; (b) sand and angular pebble with lenticular, plane, and cross bedding.

Late Pleistocene lacustrine beach deposits appear along the basin margins till elevations at least 2150–2200 m [13–15]. Lacustrine sand and silt remain best preserved in buried depressions of the paleolandscape in the northwestern and northern margins of the Chuya Basin [15]. The widespread boulders and pebbles in the Late Pleistocene lacustrine sequence on the bottom of the Chuya Depression locally formed on the moraine base by erosion of Middle Pleistocene till, while the lacustrine sediments along the margins of glacial complexes are actually redeposited glaciofluvial coarse gravels [15].

Like the cases of the Kan-Yabogan and Uimon basins, the event of abrupt lake drainage in the Chuya Basin is marked by mudflow deposits along its northern margin, at elevations between 1750 m and 1850 m corresponding to the lower part of a gently tilted piedmont plain. The belt of mudflow deposits bordering the Chuya River valley in the north has a ridge landform. Ridges mostly strike along the valley, sometimes, as transverse festooned offshoots. These deposits are mixture of waterlogged material flowing down the slopes after the dam breakthrough and the lake discharge. The sediment mixture has a heterogeneous grain size composition (Fig. 11a), from pebbles to silt, and encloses blob-like lenses or bands of light-gray sand contorted in recumbent folds, rolls, etc. The deformed layers exposed in bluff outcrops along the right tributaries of the Chuya River are flat to dipping at 40° and striking generally in the N–S direction (Fig. 11b). The deposits look like till, though having actually no relation to moraines. It is easy to confuse their primary sedimentation structures, with deformations arising from seismic-induced liquefaction and fluidization of soft sediments with different moisture contents.

The Chuya and Chuya-Kurai paleolake systems were considered [16] to be best represented by the Chagan-Uzun sequence of plane-bedded silt and sand which were deposited in proglacial lakes produced by a former glacier and were separated by several terminal moraines from the remainder Chuya Basin (Fig. 12). Note, however, that the outcrop exposes the lacustrine deposits of the Chagan-Uzun Valley used as a pathway by a retreating mountain glacier, rather than the Chuya Basin sediments. The glacier left behind a chain of relatively small lakes which were dammed by tills and persisted long after the giant ice-dammed lake from the Chuya intermontane basin had been drained.

The available thermo-luminescence (TL) and radiocarbon (^{14}C) geochronological dates for sediments from the outcrop (Fig. 13) are controversial but all correspond to Late Pleistocene ages: 58 ± 6.7 ka (MGU, KTL-93) for loamy sand from a till; 32 ± 4 kyr (MGU, KTL-1) for lower lacustrine unit, 10 m below the surface; 30815–28305 cal year BP (MGU-IOAN-65, 0.954 probability) for charcoal from a depth of 9.5 m in plane-bedded silt and sand of the upper lake unit [17]. More recent TL dates show older ages of the Chagan-Uzun deposits [18]: 90 ± 12 ka (TL-4) and 83 ± 9 ka (TL-10) for tills; 72 ± 8 ka (TL-11) for pebbles over a till; 63 ± 7 ka (TL-5), 61 ± 7 ka (TL-6), 53 ± 12 ka (TL-7), 40 ± 5 ka (TL-8), 62 ± 7 ka (TL-13), and 74 ± 9 ka (TL-14) for deposits of moraine-dammed lakes. We obtained an OSL age of 96 ± 8 ka (RIS0-132542) for sands sampled at the outcrop base (Fig. 13).

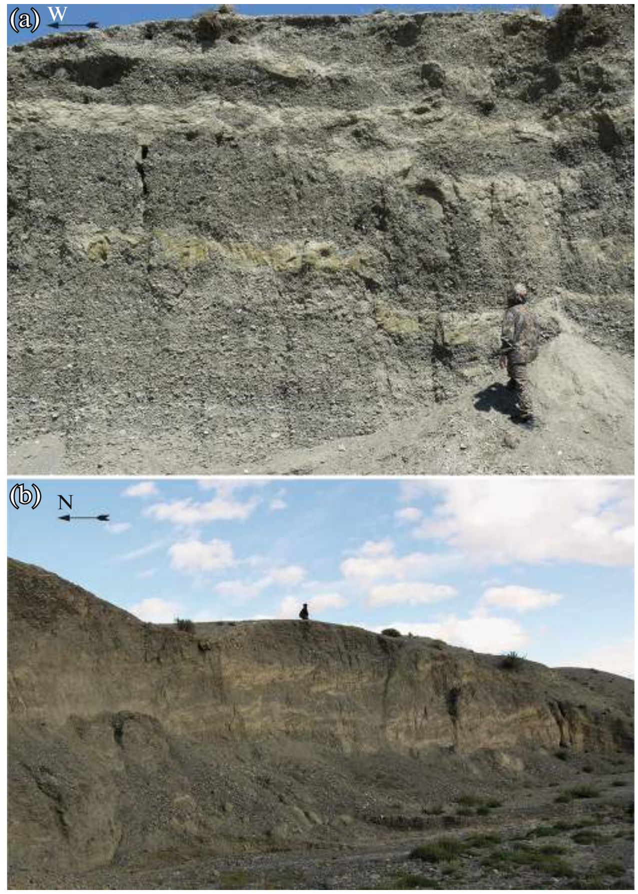

Fig. 11. Mudflow deposits along the northern margin of the Chuya Basin. (a) road excavation 6 km west of Kosh-Agach Village; (b) natural outcrop in the left side of Tozhom Creek, a right tributary of the Chuya River.

Deposits of glacial-dammed lakes of the last glaciation (marine isotope stage 2 (MIS-2)) of the Gorny Altai were established in the Kurai and Chuya basins [19–21]. On the northeastern edge of the Chuya Basin near the Kokorya Village four dates with an average age about 22 ka were obtained from lacustrine sands [21]. The level of Chuya Lake is up to 1880 m, and its depth was 140–145 m. The volume of the lake was 81 km^3 [21]. Part of the Kurai Basin was occupied in MIS-2 by the shallow Baratal Lake (the height of the shoreline is up to 1700 m) due to the fact that in the area of the Aktash Village the old and new valleys of the Chuya River were blocked by the Maashei glacier, and subsequently by its till [19, 20]. OSL dates in the age range of 21–14 ka ago were obtained from the upper part of the lacustrine parallel-bedded sands [11, 22]. The last glacial-dammed lakes in the Kurai and Chuya basins were smaller in volume than their more ancient analogues. Accordingly, the geological traces of floods from the breakthrough of glacial-dammed lakes of the MIS-2 time were significantly smaller [19, 20, 23].

Fig. 12. Fragment of Chagan-Uzun silt-sand sequence.

Fig. 13. Horizontally-bedded silt and sand deposited in a proglacial lake. Outcrop fragment.

The time when more ancient giant ice-dammed lakes disappeared from three largest intermontane basins of Gorny Altai (Fig. 1) can be inferred from the age of deposits enclosed into the glaciolacustrine and mudflow sequences or lying over megaflood deposits in the Katun and Chuya valleys. Radiocarbon and OSL dating of the aeolian and alluvial facies showed that the latest megafloods corresponding to the Saldzhar Fm. deposits in medium terraces of the Chuya and Katun rivers, which rise 60–70 m above the water table (Figs. 14a, 14b), occurred no later than 80–90 ka BP [11, 24].

Megafloods not only rushed down the Chuya and Katun valleys from the giant ice-dammed lakes through the broken dams but spilled into the Fore-Altai Plain (Ob Valley). We compare the deposits of the Last Glacial Maximum (LGM) floods of the Gorny Altai with the Bolsherechenskaya Fm. of the Fore-Altai plain [25]. We correlate the Saldzhar Fm. deposited about 90 ka BP by an Late Pleistocene megaflood (or several megafloods) with terrace IV, and the Middle Quaternary Inya Fm. (composes megaflood bars up to 300 m above the Chuya and Katun level, Figs. 14a, 14b) with terrace V of the

Fig. 14. Middle terraces (white arrow) and megaflood bars (black arrow) in the Katun (a) and Chuya (b) valleys.

Ob River (Fig. 15). The deposits from the megaflood terrace IV rise up to 80 m above the water table of the Ob River and are covered by alluvium and a subaerial complex (loess, slope wash deposits, and buried soils) of the MIS-3 stage.

Geographic information system (GIS) modeling based on the Shuttle Radar Topography Mission digital elevation model (DEM SRTM) allowed us to estimate the volume of the Ob Valley between the cities of Gorno-Altaisk and Kamen-na-Obi along the risers of terraces IV and V and to compare it with the volumes of paleolakes contoured according to wave-cut terraces of ice-dammed lakes in the Chuya and Kurai basins. The water volumes turned out to be comparable: 1055 km^3 in the Ob paleovalley and 1067 km^3 in the paleolakes of the Chuya and Kurai basins (Fig. 16). The additional 450 km^3 volume of Uimon paleolake confirms that the temporal paleolake in the Fore-Altai Plain at the flooding level till the surfaces of megaflood terraces IV and V fits the volumes of ice-dammed lakes in Gorny Altai.

These calculations exclude the possibility of hypothesizing that the volume of water in the Chuya-Kurai paleolimnic system was insufficient for the abnormally high flooding of the Ob River valley or that the waters of the giant floods spread out across the plain when they emerged from the mountains. There was no room for flatting out: the water from the Ob Valley could discharge only into depressions between ranges in the left valley side or down the Ob River into the neck near Kamen-na-Obi. The opening of the main Ob Valley into a low-lying flat plain occurs already north of Novosibirsk.

The space-time relations of megafloods with ice dams and giant ice-dammed lakes are quite obvious. Nevertheless, the paradoxic coexistence of giant current ripples and terraces in the Kurai Basin (Fig. 17) long remained unclear. The giant ripple marks would indicate catastrophic breakthrough and rapid drainage of Kurai paleolake, whereas the terraced basin side would record slow discharge without megaflood events. The paradox has several possible explanations.

The small terraced landforms may result from lateral erosion caused by catastrophic discharge of the ice-dammed lakes from the Chuya Basin. Scarps of this kind arise on the sides of modern ice-dammed lakes drained through suddenly broken dams. That was the case of the event on 11 August 2006 in the northeastern slope of Elbrus (Fig. 18) when an ice dam broke down and 400000 m^3 of water rushed out from the lake entraining 300000 m^3 of clastic material [26].

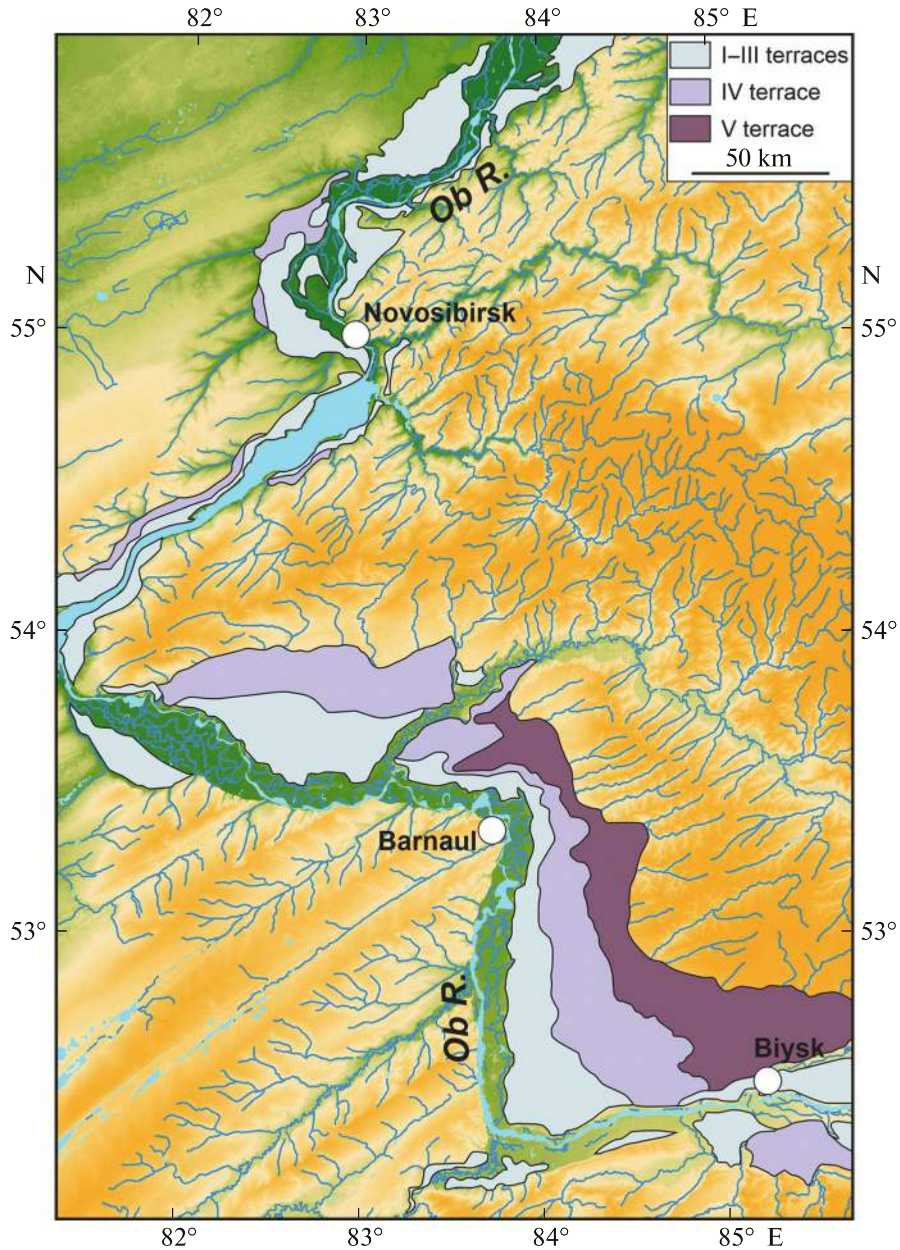

Fig. 15. Ob terraces in the Fore-Altai Plain, after [2].

Thus, the wave-cut lake shore terraces (Fig. 19a) and the small terraced landforms (Fig. 19c) differ in origin and age. The large terraces presumably cut by waves, with meters high risers and tens of meter wide surfaces, occur at 2250–2100 m asl in the Chuya Basin (Fig. 19a), whereas numerous small terraces in the 2100–1850 m interval represent the eroded upper part of a gently dipping piedmont (Fig. 19b). The small terraced landforms as in Fig. 19b have very low risers (few decimeters), extend over hundreds of meters along the basin contours, and are crosscut by downslope erosional gullies. The territory is located far from the mountains, out of the reach of any major downslope material motion, and is only exposed to fragmentary linear erosion and slow run-off. Judging by small-scale topography, the surface has preserved since the drainage of the latest paleolake and rather bears signatures of lateral erosion associated with rapid lake discharge through the broken ice dam. Larger scarps in the eastern margin of the Kurai Basin (Fig. 19c) may be related to a smaller damlake, with its level no higher than 1700 m asl, which existed during the LGM. In the same way, the giant current ripples and the terraces in the southeastern Kurai Basin (Fig. 17) may differ in age and origin.

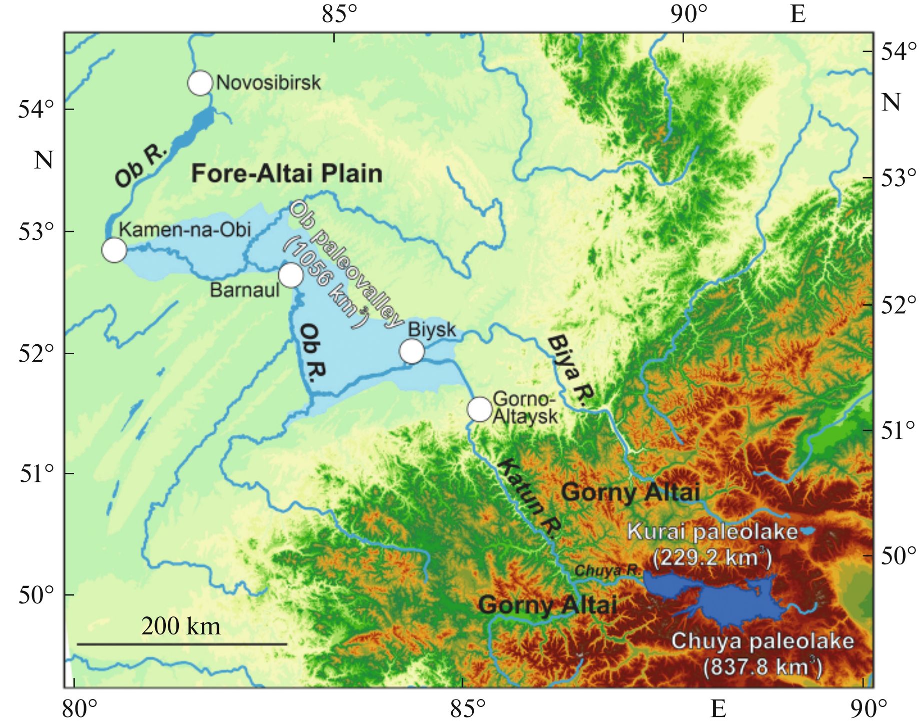

Fig. 16. Water volume modeled along the contours of terraces IV and V in the Fore-Altai Plain and the terraces of Chuya and Kurai paleolakes.

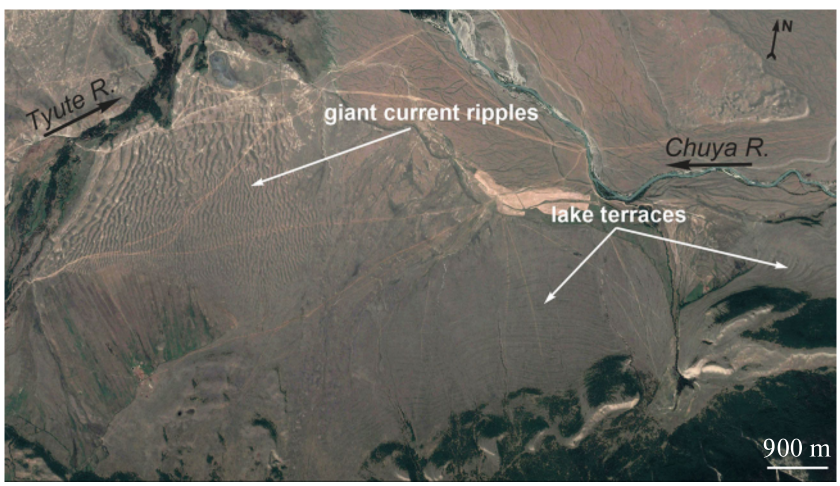

Fig. 17. Erosional terraces (right) and giant current ripples (left) in the southeastern Kurai Basin.

CONCLUSIONS

Thus, the giant ice-dammed lakes in the Uimon, Kurai, and Chuya basins of Gorny Altai arose in the Middle and twice in the Late (about 90 ka ago and in the LGM) Pleistocene. Much smaller damlakes, about the age of MIS-3–MIS-1, also formed in the three basins, as well as in the Chuya and Katun valleys, but they were rather associated with landslide and rockslide dams across major rivers or with small temporary glaciers [7, 11, 13, 27–30]. The deposits of rockslide-dammed lakes in the valleys of Katun and its side tributaries, between the Chuya and Bolshoy Yaloman rivers, have IR-OSL and OSL dates bracketed between 38 and 18 ka [11, 29].

Another lake of this kind, at least 3.5 km^3 in volume and 100 km^2 in surface area [27], formed when a giant

Fig. 18. Small terraces formed as a result of a rapidly drained modern ice-dammed lake on the Elbrus slope, after [26].

Sukor earthquake-induced rockslide induced by an earthquake dammed the Chuya Valley till the 1750–1800 m elevations [30]. The respective 1 to 4 m thick lacustrine sediments preserved in negative landforms near the dam consist of alternating yellow and yellow-gray silty sand and silt. Their OSL and TL ages indicate that the lake existed between 16 and 10 ka BP [18, 30]. The relatively low and short-living dams of MIS-2 ages in the Uimon Basin may likewise result from earthquake-induced landslide. A sample from the lowermost damlake deposits has an OSL age of 14 ± 1 ka (RIS0-132541) [11, 28].

Abrupt discharge of lakes through broken ice, landslide, or moraine dams could cause floods in the Chuya and Katun valleys about 18–14 ka ago, but their volumes and the effects of erosion, sediment transport, and terrain sculpturing were far inferior to those of the older glacial megafloods. The effect of this floods on surface topography was apparently restricted to the level of medium terraces in major river valleys.

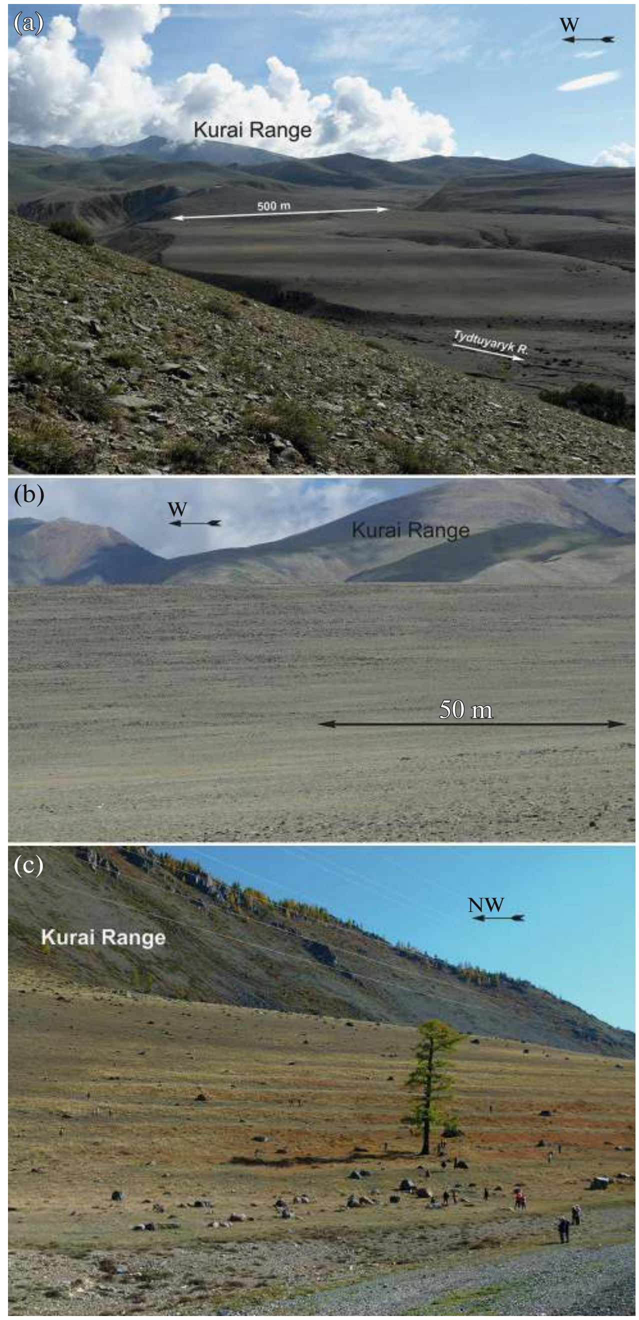

Fig. 19. Wave-cut lake terraces (a, c) and terraced piedmont slope (b) in the Chuya and Kurai basins. (a) northwestern end of the Chuya Basin (2250–2100 m asl); (b) northern side of the Chuya Basin (2100–1850 m); (c) northeastern Kurai Basin (1650–1700 m).

FUNDING

The research was carried out under a State Assignments of the V.S. Sobolev Institute of Geology and Mineralogy, Siberian Branch of the Russian Academy of Sciences (project no. 122041400252–1) and the A.A. Trofimuk Institute of Petroleum Geology and Geophysics, Siberian Branch, Russian Academy of Sciences (project no. FWZZ-2022-0001).

CONFLICT OF INTEREST

The authors of this work declare that they have no conflicts of interest.

REFERENCES

1. *The 1 : 1 000 000 State Geological Map of the Russian Federation, Map of Quaternary Deposits, New Ser., Sheet No. M-(44), 45—Ust'-Kamenogorsk,* Ed. by D. P. Avrov (Karpinsky Russ. Geol. Res. Inst., Leningrad, 1980).

2. N. V. Grigoriev, N. N. Amshinsky, L. V. Alabin, et al., *The 1 : 1 000 000 State Geological Map of the Russian Federation, New Ser., Sheet No. N-(44), 45—Novosi-*

birsk (Karpinsky Russ. Geol. Res. Inst., Leningrad, 1988).

3. I. D. Zol'nikov, A. V. Postnov, and S. A. Gus'kov, Geomorfologiya, No. 4, 75–82 (2008). https://doi.org/10.15356/0435-4281-2008-4-75-82
4. E. M. Lashkov, V. V. Kanona, and O. M. Adamenko, *The 1 : 1 000 000 State Geological Map of the Russian Federation, Altai Ser., Sheet No. M-45-VII. Explanatory Note* (Gosgeoltekhizdat, Moscow, 1961).
5. E. V. Deev, I. D. Zolnikov, and S. A. Gus'kov, Russ. Geol. Geophys. **50** (6), 546–561 (2009). https://doi.org/10.1016/j.rgg.2008.10.004
6. E. V. Deev, I. D. Zolnikov, S. V. Goltsova, et al., Russ. Geol. Geophys. **54** (3), 312–323 (2013). https://doi.org/10.1016/j.rgg.2013.02.006
7. E. V. Deev, I. D. Zolnikov, and E. Yu. Lobova, Russ. Geol. Geophys. **56** (9), 1256–1272 (2015). https://doi.org/10.1016/j.rgg.2015.08.003
8. I. D. Zolnikov and E. V. Deev, Earth's Cryosphere **17**, 74–82 (2013).
9. A. N. Uvarov, S. A. Kuznetsov, L. A. Gladkikh, et al., *The 1 : 1 000 000 Geological Map of the Russian Federation (2nd ed.), Altai Ser., Sheet No. M-45–VII (Ust'-Kan), Explanatory Note* (Karpinsky Russ. Geol. Res. Inst., St Petersburg, 2001).
10. A. N. Rudoy and G. G. Rusanov, *The Last Glaciation in Northwestern Altai* (Izd. Nauchno-Tekhn. Lit., Tomsk, 2012) [in Russian].
11. I. D. Zolnikov, E. V. Deev, S. A. Kotler, et al., Russ. Geol. Geophys. **57** (6), 933–943 (2016). https://doi.org/10.1016/j.rgg.2015.09.022
12. G. G. Rusanov, E. V. Deev, I. D. Zolnikov, et al., Russ. Geol. Geophys. **58** (8), 973–983 (2017). https://doi.org/10.1016/j.rgg.2017.07.008
13. V. V. Butvilovsky, *Paleogeography of Last Glaciation and Holocene of Altai: Event-Catastrophic Model* (Tomsk Univ., Tomsk, 1993) [in Russian].
14. G. G. Rusanov, Geomorfologiya, No. 1, 65–71 (2008). https://doi.org/10.15356/0435-4281-2008-1-65-71
15. I. D. Zol'nikov, E. V. Deev, and V. A. Lyamina, Russ. Geol. Geophys. **51** (4), 339–348 (2010). https://doi.org/10.1016/j.rgg.2010.03.002
16. P. S. Borodavko, The late Neopleistocene evolution of the Chuya–Kurai lake system, Ph.D. Thesis (Tomsk State Univ., Tomsk, 2003).
17. A. A. Svitoch, T. D. Boyarskaya, T. N. Voskresenskaya, et al., *Section of the Latest Sediments of the Altai (Key Sections of the Latest Sediments)* (Moscow State Univ., Moscow, 1978) [in Russian].
18. V. S. Sheinkman, Mater. Glyatsiol. Issled. **93**, 41–55 (2002).
19. I. D. Zolnikov, E. V. Deev, R. N. Kurbanov, et al., Geomorfol. Paleogeogr. **54** (1), 90–98 (2023). https://doi.org/10.31857/S2949178923010139
20. I. D. Zolnikov, I. C. Novikov, E. V. Deev, et al., Led Sneg **63** (4), 639–651 (2023). https://doi.org/10.31857/S207667342304018X
21. I. D. Zolnikov, I. S. Novikov, R. N. Kurbanov, et al., Limnol. Freshwater Biol., No. 4, 753–756 (2024). https://doi.org/10.31951/2658-3518-2024-A-4-753
22. I. D. Zolnikov, E. V. Deev, R. N. Kurbanov, et al., Dokl. Earth Sci. **496** (2), 176–181 (2021). https://doi.org/10.1134/S1028334X21020227
23. A. R. Agatova, R. K. Nepop, P. A. Carling, et al., Earth-Sci. Rev. **205**, 103–183 (2020). https://doi.org/10.1016/j.earscirev.2020.103183
24. M. I. Svistunov, R. N. Kurbanov, A. S. Murray, et al., Quat. Geochronol. **73**, 101399 (2022). https://doi.org/10.1016/j.quageo.2022.101399
25. I. D. Zolnikov, E. A. Filatov, A. V. Shpansky, et al., Geomorfol. Paleogeogr., No. 4, 13–26 (2024). https://doi.org/10.31857/S2949178924040023
26. S. S. Chernomorets, D. A. Petrakov, O. V. Tutubalina, et al., Mater. Glyatsiol. Issled. **102**, 211–215 (2007).
27. G. G. Rusanov, Vopr. Geogr. Sib. **22**, 18–25 (1997).
28. E. V. Deev, I. D. Zolnikov, I. V. Turova, et al., Russ. Geol. Geophys. **59** (4), 437–452 (2018). https://doi.org/10.1016/j.rgg.2017.07.011
29. E. Deev, I. Turova, A. Borodovskiy, et al., Quat. Sci. Rev. **203**, 68–89 (2019). https://doi.org/10.1016/j.quascirev.2018.11.009
30. E. V. Deev, I. D. Zolnikov, R. N. Kurbanov, et al., Russ. Geol. Geophys. **63** (6), 743–754 (2022). https://doi.org/10.2113/RGG20204300

Publisher's Note. Pleiades Publishing remains neutral with regard to jurisdictional claims in published maps and institutional affiliations.
AI tools may have been used in the translation or editing of this article.